Int. J. Electrochem. Sci., 13 **(2018)** 9007 – 9016, doi; 10.20964/2018.09.67

International Journal of
ELECTROCHEMICAL
SCIENCE
www.electrochemsci.org

Ball-like Pt Nanoparticles on GO-modified Carbon Fiber Cloth with High Electrocatalytic Activity for Methanol Oxidation

Fang Lu[1,2], *Chunyong Zhang*[1,2,*], *Jiehong Cheng*[2,3,*], *Cheng Zhu*[1,2], *Haojing Zhang*[1,2], *Xian Cheng*[2,3]

[1] Jiangsu Key Laboratory of Precious Metal Chemistry and Technology, Jiangsu University of Technology, Changzhou, 213001, China
[2] School of Chemistry and Environmental Engineering, Jiangsu University of Technology, Changzhou, 213001, China
[3] Jiangsu Province Key Laboratory of E-Waste Recycling, Jiangsu University of Technology, Changzhou, 213001, China
Fang Lu, Chunyong Zhang, Jiehong Cheng contributed equally to this article.
[*]E-mail: zhangcy@jsut.edu.cn, cjh@jsut.edu.cn

Received: 24 May 2018 / *Accepted:* 30 June 2018 / *Published:* 5 August 2018

A direct methanol fuel cell (DMFC) electrode based on the carbon fiber cloth (CFC) modified with wrap-like graphene oxide (GO) decorated with platinum nanoparticles was prepared by multicycle CV method. Also, the Pt/CFC composite and GO/CFC composite were prepared by multicycle CV and potentiostatic method, respectively. The four electrodes (GO-Pt/CFC, Pt/CFC, GO/CFC and CFC) were tested in a fuel cell for electro-oxidation of methanol and were analyzed by scanning electron microscopy (SEM) and X-Ray powder diffraction (XRD). The SEM image indicated that the surface of CFC was covered by a wrap-like graphene oxide (GO) film completely, which increased the contact area with methanol solution and provided more load points. And the Pt nanoparticles supported GO/CFC electrode possessed the ball-like morphology. The electrochemical measurements showed that the electrocatalytic peak current density of methanol oxidation of GO-Pt/CFC electrode (218 mA/cm^2) was about 27% higher than Pt/CFC electrode (172 mA/cm^2) and the steady-state current density of GO-Pt/CFC electrode was 57.6%, 114.5% and 497.9% higher than that of Pt/CFC, GO/CFC and CFC electrodes, respectively. And this date revealed that the ball-like morphology of Pt nanoparticles and a wrap-like GO film coated on CFC surface were favorable to improve the electrocatalytic oxidation activity of methanol.

Keywords: Direct Methanol Fuel Cell; Graphene Oxide; Pt nanoparticles; Electro-catalytic Activity; Carbon Fiber Cloth

1. INTRODUCTION

Due to the increasing energy crisis and environmental pollution, the development of efficient and clean new energy is becoming more and more urgent and significant[1-2]. The direct methanol fuel cell has a wide application prospect in the portable mobile power supply because of the advantages of convenient carrying, simple structure, high theoretical specific energy, and abundant fuel resources[3-4]. However, the major weakness of direct methanol fuel cell commercialization because it has difficult in electrocatalyst preparation and methanol permeation[5]. People widely use Pt-based catalysts as excellent electrodes for the DMFC because that they have high catalytic activity and power densities for methanol oxidation[6-7]. Nevertheless, low content in nature and non-renewable are the major weakness of Pt as methanol fuel cell catalyst. Furthermore, the methanol oxidation intermediate product (such as CO) is easily adsorbed on the surface of metal Pt catalyst, resulting in its adsorption and dissociation difficultly[8-9]. Therefore, it leads to the Pt catalyst with lower utilization and it has seriously limited the commercial application of direct methanol fuel cells[10-11]. Improving catalyst utilization to reduce costs, preparing Pt-based metal composite catalysts, finding new non-precious metal catalysts, and seeking new catalyst carriers are the current research hotspot and direction. And the development of the catalyst with high electrochemical activity, long life, and low cost remains a hot topic in methanol fuel cell catalysts.

Graphene is a two-dimensional carbon material, with the carbon atoms arranged in a hexagon-shaped lattice[12]. The advent of graphene has caused a worldwide study craze. At present, graphene is the thinnest but also the hardest two-dimensional material in the world[13]. Owing to its excellent performance, low cost, high surface area, superior electrical conductivity, and chemical stability, it has become a new choice as a precious metal catalyst substrate. Graphene has low resistivity and fast electron transfer. Essentially, as good transparent conductor with a high surface area, graphene is suitable for the manufacture of transparent electrodes and touch screen. In addition, it is also widely used in the field of new energy materials[14]. Graphene is currently the thinnest material with a thickness of about 0.34 nm and has the highest strength among the known materials at 130 GPa, more than 100 times stronger than steel. The carrier mobility of the graphene up to 1.5×10^4 $cm^2/V\cdot S$, more than 10 times of commercial silicon wafers[15-16]. The thermal conductivity of graphene can reach 5.3×10^3 W/m·K, much higher than that of single-wall (3.5×10^3 W/m·K) and multi-wall (3.0×10^3 W/m·K) carbon nanotubes[17].

In the present work, to improve the methanol utilization and catalyst activity of DMFC, a 3D electrode of GO decorated with Pt nanoparticles was made by multicycle CV and potentiostatic method. The structural characterization method that we applied during our investigation were: scanning electron microscopy (SEM) and X-Ray powder diffraction (XRD). The effect of Pt and GO addition on the kinetics of methanol electro-oxidation reaction was researched by cyclic voltammetry, chronoamperometry, and impedance measurements on CFC, GO/CFC, Pt/CFC and GO-Pt/CFC electrodes.

2. EXPERIMENTAL

2.1. Chemicals

Nitric acid (HNO_3), Sulfuric acid (H_2SO_4), Methanol (CH_3OH) and Ethanol (C_2H_5OH) were obtained from Sinopharm Chemical Reagent Co., Ltd. Chloroplatinic acid hexahydrate ($H_2PtCl_6\cdot6H_2O$)

and Graphene oxide (GO) dispersion were purchased from Aladdin and XFNANO, respectively.

2.2 CFC pretreatment

Carbon Fiber Cloth (CFC) was used as substrate for preparation of GO/CFC, Pt/CFC and GO-Pt/CFC electrodes. The untreated CFC needs to be pretreated, because of its hydrophobic property. Thus, the graphene oxide and Pt particles are better supported the CFC. In total, the CFC (0.8 cm×1 cm) and 100 mL nitric acid (20 wt%) were added to a round bottom flask (250 mL), which was soaked in an oil bath under continuously stirring at 70 °C for 6 h. After the mixer was cooled down to 20 °C, the CFC was washed with acetone and distilled water and dried at room temperature.

2.3 Electrodes preparation

Electrodes were executed in a conventional three-electrode cell with Pt wire as a counter electrode and saturated calomel electrode as a reference electrode with a CHI760E electrochemical workstation. The working electrode was a the pretreated CFC. The GO/CFC electrode was prepared at -1.2 V with a run time of 60000s in 2 mg/mL GO solution by potentiostatic method, and the Pt/CFC and GO-Pt/CFC electrodes were prepared between -0.4 V and 1.3 V with a scan rate of 50 mV/s in 0.5 M H_2SO_4 + 0.005 M H_2PtCl_6 by multicycle CV method at room temperature.

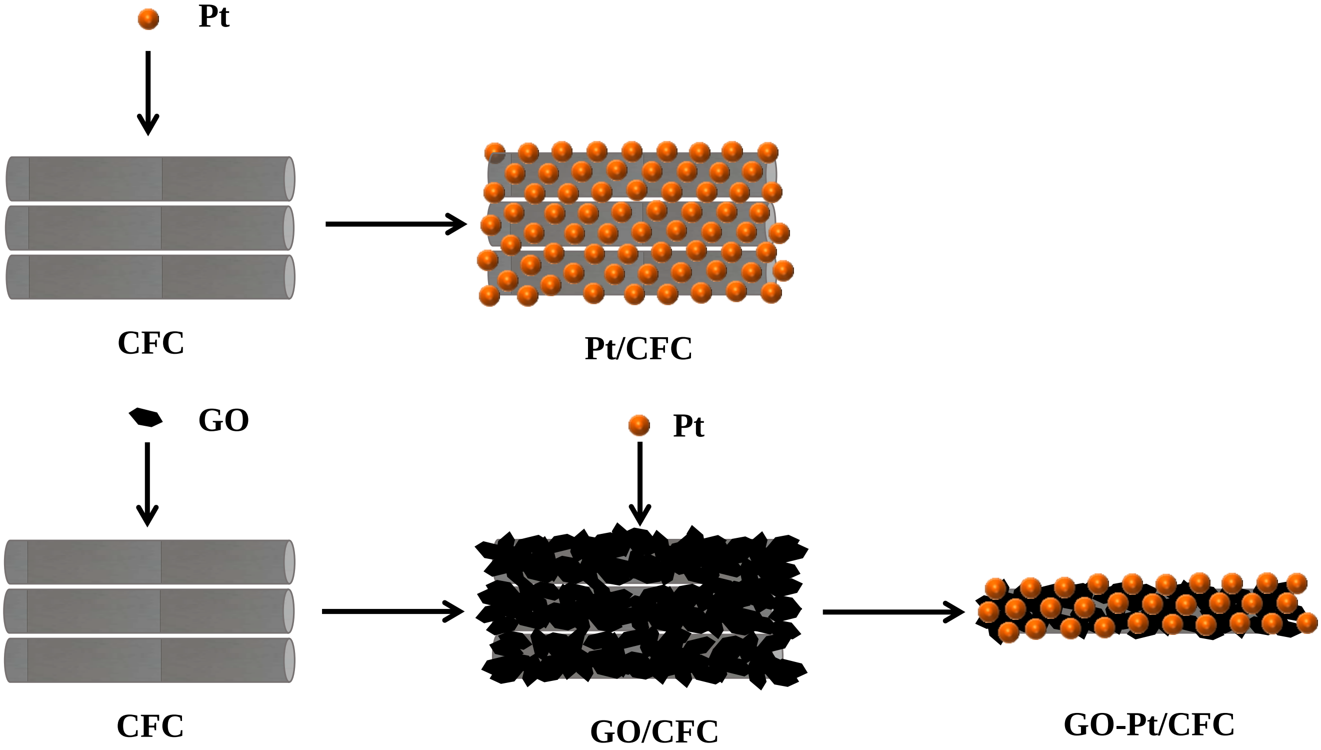

Figure 1. Schematic illustration of Pt/CFC, GO/CFC and GO-Pt/CFC electrodes preparation.

3. RESULTS AND DISCUSSION

Because of high carrier mobility and excellent chemical stability, graphene has been widely used as electrode material for methanol fuel cells. The carbon-based materials supported Pt/GO nanocomposite catalyst have been widely studied, including Pt/MOGO (Pt/mildly oxidized graphene oxide)[18], Pt@GO-PVPNPs (Pt@GO-polyvinylpyrrolidone nanoparticles)[19], GNP/Pt (graphene nanoplate-Pt)[20], Ru@Pt/GOCNT (Ru@Pt/graphene-carbon nanotube)[21], Pt/CNx (Pt/graphitic carbon nitride)[22], Ni@Pt/MWCNTs (Ni@Pt/multi-walled carbon nanotubes)[23], Pt/GO (Pt/graphene oxide)[24]. And Table 1 summarizes the manifold Pt nanocomposite catalyst mentioned above.

Table 1. The carbon-based materials supported Pt catalyst for methanol electrooxidation

Electrode Material	Electrochemical testing equipment	Test Solutions	Specific power/Mass activity	Reference
Pt/MOGO	Chi-600e	0.5 M H_2SO_4 + 1 M CH_3OH	0.33 mW/mgPt	[18]
Pt@GO-PVPNPs	/	0.5 M H_2SO_4+0.5 M CH_3OH 50 mV/s	43 mA/cm^2	[19]
GNP/Pt	CHI 660B	1 M H_2SO_4+2 M CH_3OH 20 mV/s	57.7 mA/cm^2	[20]
Ru@Pt/GOCNT	CHI600e	1 M KOH+1 M CH_3OH	13.1 mW/mgPtRu	[21]
Pt/CNx	/	1 M H_2SO_4+1 M CH_3OH 20 mV/s	310 mA/mgPt	[22]
Ni@Pt/MWCNTs	Potentiostat/Galvanostat	0.5 M H_2SO_4+0.5 M CH_3OH 50 mV/s	216.7 mA/mgPt	[23]
Pt/GO	ECW-5000	0.5 M H_2SO_4+1 M CH_3OH 20 mV/s	4.3 mA/cm^2	[24]
GO-Pt/CFC	CHI760E	0.5 M H_2SO_4+0.5 M CH_3OH 50 mV/s	218 mA/cm^2	This work

Fig. 2 shows the SEM images of the CFC, GO/CFC , Pt/CFC and GO-Pt/CFC electrodes. It can be observed that the CFC electrode surface is very smooth. Three-dimensional and thin nano-filmed structure of GO/CFC electrode can be clearly observed in Fig. 2B. The GO nano-film not only provided a better platform for the subsequent deposition of Pt particles but also increased the contact area with the electrolyte. As shown in Fig. 1C, the Pt nanoparticles deposited on CFC exhibit a typical platelet-like morphology with several three-dimensional crystallites. The Fig. 1D shows that Pt nanoparticles are highly dispersed on three-dimensional GO/CFC surface. The Pt nanoparticles deposited on the surface of GO/CFC display a dense three-dimensional ball-like structure.

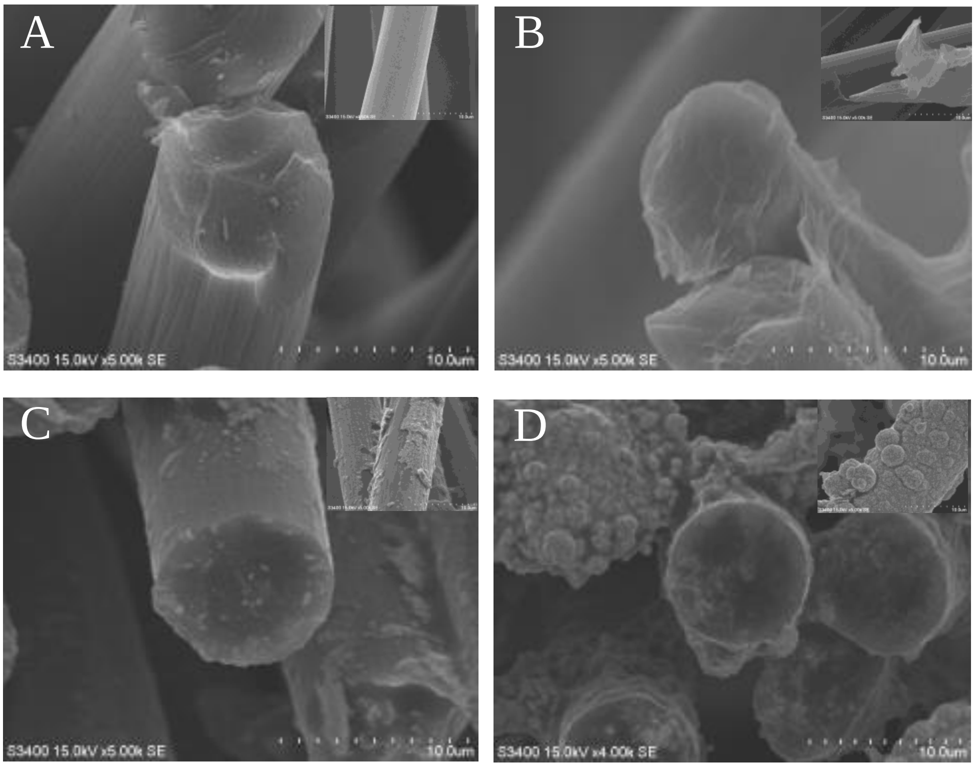

Figure 2. SEM images of (A) CFC, (B) GO/CFC,(C) Pt/CFC, (D) GO-Pt/CFC electrodes.

Fig. 3 illustrates the diffractograms of the X-ray diffraction (XRD) patterns of CFC, GO/CFC, Pt/CFC and GO-Pt/CFC nano composites electrodes. XRD patterns of as-prepared electrodes were recorded on D/MAX-2500PC (Rigaku Miniflex II) Instrument using Cu Kα radiation (λ = 1.5406 Å) with the scattered angle range of 5° to 90°, operating at 40 kV and 40 mA. It can be seen obviously that CFC exhibit an amorphous structure identified by a characteristic diffraction peak at about 2θ = 25.9° and 43.9° that are related to the C (002) and (100) planes. After electrodepositing of GO, the significant diffraction peak emerges around 2θ = 10.5° corresponding to GO (002). The Pt-GO/CFC diffractogram shows five peaks around 2θ = 39.5°, 46.1°, 67.5°, 81.5° and 85.9°. Draw on the previous reports, we can see mainly five peaks for nano Pt particles[25], around 2θ = 39.5°, 46.1°, 67.5°, 81.5° and 85.9° assigned to the (111), (200), (220), (311) and (222) planes for Pt particles. These five characteristic diffraction peaks show that Pt particles possess a face-centred cubic structure[26-27] in Pt-GO/CFC and Pt/CFC electrodes. The positions of the peaks were consistent with JCPDS Card 01-1994.

Fig. 4 shows the CVs of the CFC, GO/CFC, Pt/CFC and GO-Pt/CFC electrodes in 0.5 M H_2SO_4 and 0.5 M CH_3OH solution with a scan rate of 50 mV/s. As we can seen in this image. the GO-Pt/CFC electrode has a strong methanol oxidation peak at the potential sweep, with a peak potential of 1.12 V and an oxidation peak at 0.70 V when the potential sweep was negative. Similarly, the Pt/CFC electrode has an oxidation peak at 0.92 V in the forward scan, and an oxidation peak at the negative scan of 0.53 V. Compared with the GO-Pt/CFC electrode and the Pt/CFC electrode, the CFC and the GO/CFC electrodes oxidation peak can be neglected.

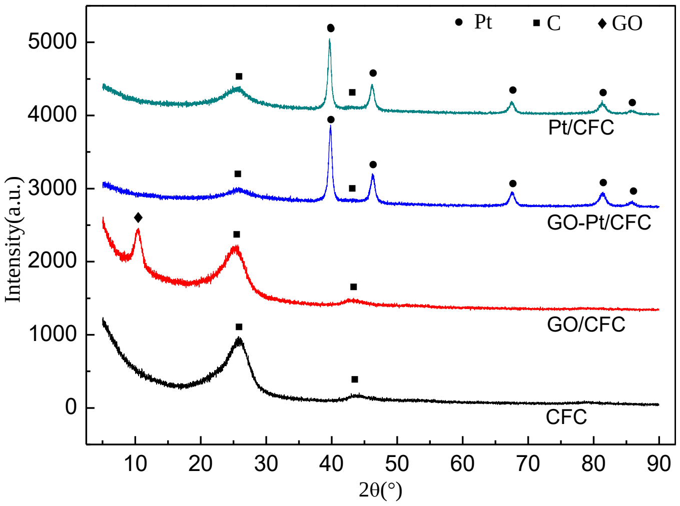

Figure 3. XRD patterns of CFC, GO/CFC, Pt/CFC and GO-Pt/CFC electrodes.

It is generally believed that the posgitive peak (I_f) is related to the oxidation of methanol while the negative peak (I_b) is related to the reaction of the methanol intermediate because the oxidation of methanol is a multi-step reaction[28-29]. And the ratio of I_f/I_b is used to measure the catalyst which is the ability to resist poisoning, the larger of the ratio, the stronger the anti-poisoning ability of the catalyst[30-31]. As we can see from the cyclic voltammogram image, the ratio of I_f/I_b indicated that the GO-Pt/CFC electrode (1.11) is higher than Pt/CFC electrode (1.08). However, it was obvious that the oxidation peak current density of the GO-Pt/CFC electrode and the Pt/CFC electrode varies significantly with the potential in methanol solution. As GO was added, it can be seen that the GO-Pt/CFC electrocatalyst has a better catalytic performance for methanol oxidation than the Pt/CFC electrode. The positive peak current density is 218 mA/cm^2, which is 46 mA/cm^2 more than the positive peak current density of the Pt/CFC electrode (172 mA/cm^2).

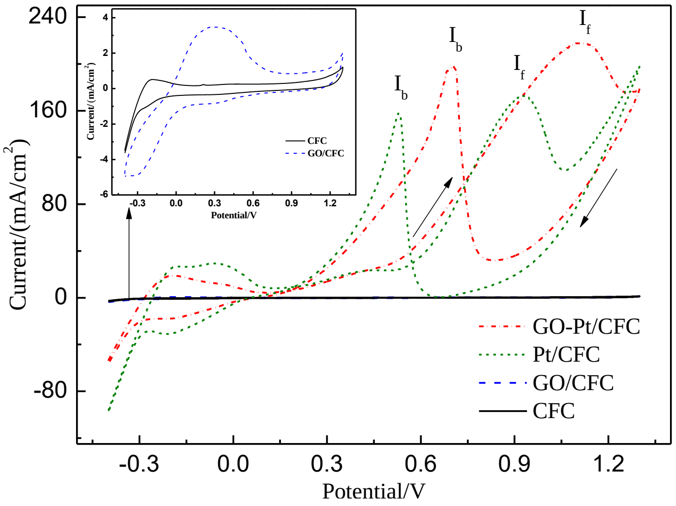

Figure 4. The cyclic voltammograms of CFC, GO/CFC, Pt/CFC and GO-Pt/CFC electrodes at a scan rate of 50 mV/s in 0.5 M CH_3OH and 0.5 M H_2SO_4 solution at room temperature.

Fig. 5 shows the amperometric i-t curve of these four electrodes in 0.5 M H_2SO_4 and 0.5 M

CH_3OH solution. From the amperometric i-t curve, there is a large current drop at the initial phase and then gradually stabilized over time. After 600 s, the GO-Pt/CFC, Pt/CFC, GO/CFC and CFC electrodes of methanol catalytic oxidation current density are 0.112 mA/cm^2, 0.071 mA/cm^2, 0.054 mA/cm^2 and 0.018 mA/cm^2, respectively. As can be seen from the Fig. 5, after 600 s reaction of the GO-Pt/CFC electrode, the steady current density is much higher than the other three electrodes. It is probably due to the better dispersibility of Pt nanoparticles deposited on the surface of GO/CFC electrode, which resulted in the higher catalytic activity after 600 s.

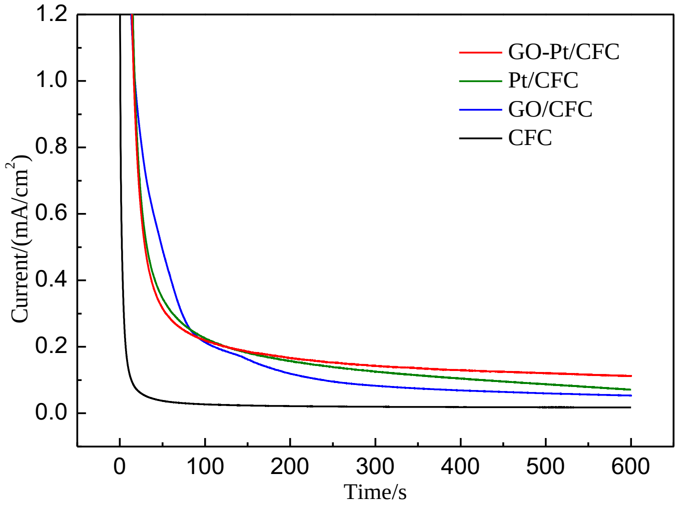

Figure 5. Chronoamperometry curves of CFC, GO/CFC, Pt/CFC and GO-Pt/CFC electrodes in 0.5 M H_2SO_4 and 0.5 M CH_3OH solution at room temperature.

Fig. 6 shows the multi-turn CV images of the CFC, GO/CFC, Pt/CFC and GO-Pt/CFC electrodes in 0.5 M H_2SO_4 and 0.5 M CH_3OH solution with a scan rate of 50 mV/s. At the 10th cycle, the current density reached the maximum value which is 288.8 mA/cm^2 and then gradually decreased with the number of cycles. Compared the multi-turn CV images of four electrodes, GO-Pt/CFC electrode has higher steady current density, which indicated that the GO-Pt/CFC electrode has excellent stability of methanol oxidation. And the result was consistent with the amperometric i-t curve.

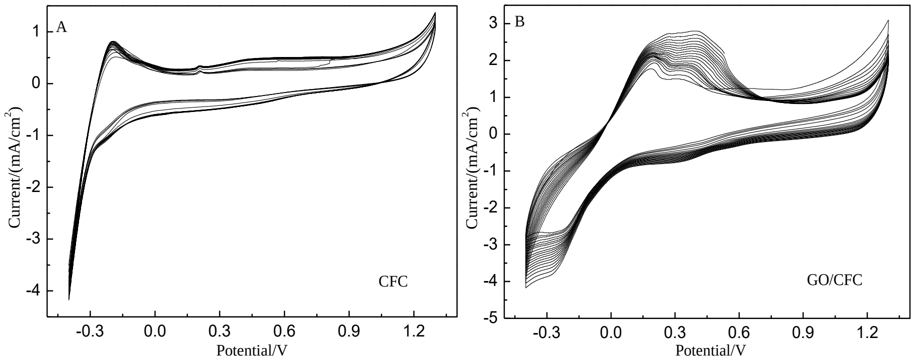

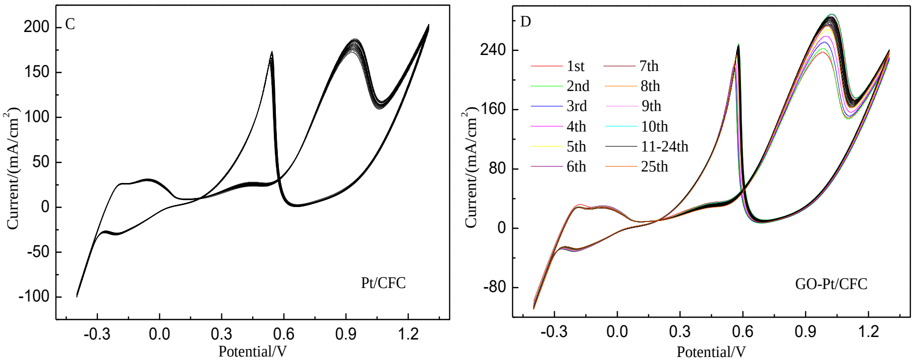

Figure 6. The multi-turn cyclic voltammograms of A) CFC, B) GO/CFC, C) Pt/CFC and D) GO-Pt/CFC electrodes at a scan rate of 50 mV/s in 0.5 M CH_3OH and 0.5 M H_2SO_4 solution for 25 cycles.

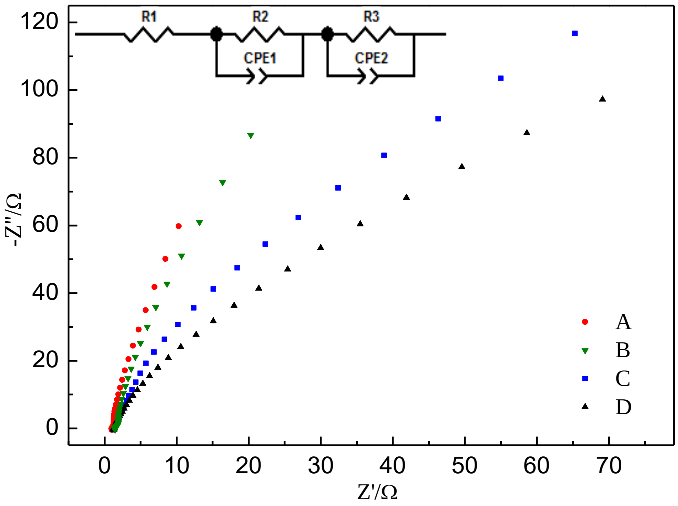

Figure 7. The electrochemical impedance spectroscopy at -0.2 V for the methanol fuel cell in 0.5 M H_2SO_4 and 0.5 M CH_3OH solution at room temperature. A) GO-Pt/CFC, B) Pt/CFC, C) GO/CFC, D) CFC.

Fig. 7 shows the Nyquist plots of the CFC, GO/CFC, Pt/CFC and GO-Pt/CFC electrodes in 0.5 M H_2SO_4 and 0.5 M CH_3OH solution. It can be seen from Fig. 7 that the different shapes of electrochemical impedance spectroscopy were obtained for CFC and modified GO/CFC, Pt/CFC and GO-Pt/CFC electrodes in 0.5 M H_2SO_4 and 0.5 M CH_3OH solution. The inset in the Fig. 7 is the equivalent circuit. Obviously, the impedance arc radius of the GO-Pt/CFC electrode is larger than others. It was observed that the sequence of impedance arc radius of electrodes follows the sequence GO-Pt/CFC > Pt/CFC > GO/CFC > CFC. Generally speaking, the larger resistance of GO-Pt/CFC electrode which can be seen as a series circuit with the dense 3D nanostructure of Pt particle layer, the GO with high surface area layer and the CFC. Therefore, the charge transfer resistance and rate become larger and more slowly, respectively.

4. CONCLUSION

The GO and Pt particles were successfully deposited on the CFC surface by potentiostatic and multicycle CV methods, respectively. In physically characterize, the GO has three-dimensional nano-filmed structure, and the Pt nanoparticles have platelet-like morphology. In the electrochemical test, the GO-Pt/CFC electrode far outperformed GO/CFC, Pt/CFC, and CFC electrodes regarding both electrochemical activity and stability. It was found that the best electro-activity property was achieved for Pt particles electrodeposited on GO/CFC surface in scan rate of 50 mV/s. Moreover, it is confirmed by our study that GO-Pt/CFC electrode with three-dimensional ball-like morphology produced by potentiostatic and multicycle CV deposition methods can be used as an efficient electrode in DMFC.

ACKNOWLEDGEMENT
This work was supported by National Key Technology Support Program of China (Grant No. 2014BAC03B06), Natural Science Foundation of the Jiangsu Higher Education Institutions of China (15KJA610001), Research Institutes Association Innovative Program of Jiangsu Province (BY2016030-09), and Postgraduate Research & Practice Innovation Program of Jiangsu Province (20820111739).

References

1. A.V. Bidder, *Best Life*, 102 (2009) 30.
2. B. Grievson, *Blackwell Science Ltd*, (2007) 466.
3. B. Kuppan and P. Selvam, *Progress in Natural Science: Materials International*, 22 (2012) 616.
4. D. E. Glass, G. A. Olah and G. K. S. Prakash, *Journal of Power Sources*, 352 (2017).
5. J.-M. Jehng, W.-J. Liu, T.-C. Pan and Y.-M. Dai, *Applied Surface Science*, 268 (2013) 425.
6. C. Alegre, D. Sebastián, M. E. Gálvez, R. Moliner and M. J. Lázaro, *Applied Catalysis B: Environmental*, 192 (2016) 260.
7. L. Y. Zhong, Y. G. Bao, C. X. Li, Y. Y. Qin and B. Liu, *Chemical Engineering Journal*, 161 (2010) 27.
8. S. Shironita, K. Sato, K. Yoshitake and M. Umeda, *Electrochimica Acta*, 206 (2016) 254.
9. E. Negro, R. Latsuzbaia, M. Dieci, I. Boshuizen and G. J. M. Koper, *Applied Catalysis B: Environmental*, 166-167 (2015) 155.
10. W. Yuan, Y. Zhang, N. Zhang, C. Yin, X. Zhang and X. Liu, *Catalysis Communications*, 100 (2017).
11. L. I. Min, Y. Luo, X. U. Wei-Jia and J. X. Liu, *Journal of Inorganic Materials*, 32 (2017) 916.
12. A. K. Geim and K. S. Novoselov, *Nature Materials*, 6 (2007) 183.
13. C. Lee, X. Wei, J. W. Kysar and J. Hone, *Science*, 321 (2008) 385.
14. M. Pumera, *Energy & Environmental Science*, 4 (2011) 668.
15. J. H. Chen, C. Jang, S. Xiao, M. Ishigami and M. S. Fuhrer, *Nature Nanotechnology*, 3 (2008) 206.
16. M. D. Stoller, S. Park, Y. Zhu, J. An and R. S. Ruoff, *Nano Letters*, 8 (2008) 3498.
17. K. S. Novoselov, Z. Jiang, Y. Zhang, S. V. Morozov, H. L. Stormer, U. Zeitler, J. C. Maan, G. S. Boebinger, P. Kim and A. K. Geim, *Science*, 315 (2007) 1379.
18. Y. H. Kwok, A. C. H. Tsang, Y. Wang and D. Y. C. Leung, *Journal of Power Sources*, 349 (2017) 75.
19. Z. Daşdelen, Y. Yıldız, S. Eriş and F. Şen, *Applied Catalysis B:environmental*, 219 (2017) 511.
20. H. Huang, H. Chen, D. Sun and X. Wang, *Journal of Power Sources*, 204 (2012) 46.
21. Y. H. Kwok, Y. F. Wang, A. C. H. Tsang and D. Y. C. Leung, *Applied Energy*, 217 (2018) 258.

22. M. Sadhukhan, M. K. Kundu, T. Bhowmik and S. Barman, *International Journal of Hydrogen Energy*, 42 (2017) 9371.
23. S. Ali, I. Khan, S. A. Khan, M. Sohail, R. Ahmed, A. U. Rehman, M. S. Ansari and M. A. Morsy, *Journal of Electroanalytical Chemistry*, 795 (2017) 17.
24. J. M. Jehng, W. J. Liu, T. C. Pan and Y. M. Dai, *Applied Surface Science*, 268 (2013) 425.
25. Y. Wang, Q. Cheng, T. Yuan, Y. Zhou, H. Zhang, Z. Zou, J. Fang and H. Yang, *Chinese Journal of Catalysis*, 37 (2016) 1089.
26. F. A. Viva, G. A. Olah and G. K. S. Prakash, *International Journal of Hydrogen Energy*, (2017).
27. Q. Zhou, G. C. Wang, L. Yang, Y. Yang and Y. Xu, *Applied Mechanics & Materials*, 320 (2013) 670.
28. M. Li, G. Han, B. Yang, Y. Chang, Y. Xiao and Y. Li, *Catalysis Communications*, 51 (2014) 86.
29. D. Wang, *Journal of Colloid & Interface Science*, 367 (2012) 199.
30. L. Zhang and D. Xia, *Acta Physico-chimica Sinica*, 252 (2005) 2191.
31. L. Dong, R. R. S. Gari, Z. Li, M. M. Craig and S. Hou, *Carbon*, 48 (2010) 781